Biointerface Research in Applied Chemistry
Open-Access Journal (ISSN: 2069-5837)

Article
Volume 13, Issue 3 2023, 215
https://doi.org/10.33263/BRIAC133.215

Virtual Screening and Molecular Docking of Flavone Derivatives as a Potential Anticancer Drug in the Presence of Dexamethasone

Akash Bhattacharya [1,2], Priyanka Sen Guha [3], Nilkanta Chowdhury [4], Angshuman Bagchi [4], Dipanjan Guha [1,*]

1 S. N. Bose Innovation Centre, University of Kalyani, Kalyani, West Bengal, India
2 Calcutta School of Tropical Medicine, Kolkata, West Bengal, India
3 Department of Biotechnology, Brainware University, Barasat, West Bengal, India
4 Department of Biochemistry and Biophysics, University of Kalyani, Kalyani, West Bengal, India
* Correspondence: dipanjaninvc18@klyuniv.ac.in (D.G.);

Scopus Author ID 51863398600
Received: 5.03.2022; Accepted: 18.04.2022; Published: 5.06.2022

Abstract: CDK6 is a pivotal kinase in cell cycle progression and has been targeted in many cancers and degenerative diseases. Fisetin, a potent flavonol inhibitor of CDK6, was modified *in silico* to develop better CDK6 inhibitor(s). Molecular docking studies were performed with *in silico*-derived fisetin derivatives. All fisetin derivatives were capable of being CDK6 inhibitors; two of them had improved binding characteristics compared to fisetin. Molecular docking studies were executed in the presence of dexamethasone, a commonly administered corticosteroid. These two derivatives showed a stronger binding affinity with CDK6 in the presence of dexamethasone. Two fisetin derivatives had a thermodynamically favorable interaction with CDK6 compared to fisetin and had equivalent ADME properties, and would be well tolerated by the body. This study holds immense potential for developing new flavonoid drugs for cancer.

Keywords: flavones; dexamethasone; anticancer drugs; in silico drug designing; molecular docking.

1. Introduction

Molecular docking is a powerful tool in computer-based drug design. It is an important technique for predicting protein-small molecule interactions. The information generated from the output of molecular docking can predict the binding of small molecules with protein [1]. Free energy of binding can predict the stability of the protein-ligand complex in different conformations [2,3]. In modern science, molecular docking has revolutionized the drug discovery process and can be explored to investigate anticancer drugs.

Cyclin-dependent kinases (CDKs) are a group of critical regulatory enzymes which regulate all cell cycle processes [4]. Proper expression of these kinases is tightly regulated, and their timely activation maintains cell homeostasis [5]. Altered expression of CDKs, including CDK4 and/or CDK6, can lead to malignancy [6,7]. Small molecules, including various flavonoids, have been proven to have potential as CDK6 inhibitors.

Some flavonoids have well-established anticancer properties [8]. Plants are the main source of flavonoids, and their extraction from tea leaves, cocoa powder, plums, etc., has already been reported [9]. All naturally found flavonoids are reported to have antioxidant

properties [9], and most of them can stimulate an anti-inflammatory response and exhibit strong anticancer properties [9]. Flavopiridol (Alvocidib), a synthetic flavonoid, was the first CDK inhibitor to be investigated in clinical trials. However, its limited therapeutic efficiency and undesirable toxicity profile prevented its use as a single agent therapeutic. [10]. Then came the second generation of non-flavonoid drugs like AG-024322, dinaciclib, AT7519, AZD5438, etc. [10]. Ribociclib, palbociclib, and flavonoids (like apigenin, fisetin (FL), chrysin), etc., are currently being researched as CDK4/6 inhibitors. The third generation drugs show good performance against the patients suffering from breast and non-small cell lung cancer.

Dexamethasone (DXM), a glucocorticoid [11], has shown promise in cancer treatment [12]. It is an anti-inflammatory drug that can suppress body's immune response [12]. DXM is mainly used as an anti-emetic during cancer therapy. Recently, it has been shown that DXM treatment can increase antitumor activity [12]. For example, DXM acts synergistically with ribociclib (a CDK6 inhibitor) to elevate its antitumor response [13]. This result encouraged us to hypothesize that the efficacy of *in silico* synthesized flavonoids as CDK6 inhibitors may be enhanced in the presence of DXM.

To date, different strategies have been implemented to stall cancer progression [14–16] and designing an efficient inhibitor of CDK6 is one of them. However, lack of specificity, drug resistance, and toxicity has prevented their translation into effective therapeutic agents. This report investigated the efficacy of several flavonoids synthesized through *in silico* modeling as CDK6 inhibitors in the presence and absence of DXM. Our results suggest that the binding affinity of two of these compounds is enhanced in the presence of DXM, and their combination may be considered for therapy. These preliminary findings might be useful in discovering novel anticancer agents in the near future.

2. Materials and Methods

2.1. Collection and preparation of ligands.

The 3D structure of FL, its derivatives (FL-D1, FL-D2, FL-D3, FL-D4, FL-D5, FL-D6, FL-D7, FL-D8, FL-D9, and FL-D10), and DXM were drawn using ACD/ChemSketch software. The parent ligand (FL) was structurally modified, keeping the backbone intact to obtain its derivatives. Extra –OH groups were incorporated in different positions of a benzene ring, and one and/or two –Cl groups were added in different positions to the parent ligand. Energy minimization of DXM, FL, and its derivatives (FL-D1 to FL-D10) was executed in chem3D pro 12.0 to get the optimum geometric conformation. All the ligands were prepared in PDB format for further analysis.

2.2. Collection and preparation of macromolecules.

The RCSB PDB homepage was used to download the crystal structure of the target protein CDK6 (PDB ID: 5L2I) [17]. The protein molecule was prepared for further analysis. PYMOL (version 2.4.2) removed the unwanted ligand from CDK6. The structure was then energy minimized using the 'energy minimization' protocol of Swiss-PdbViewer 4.1.0 using GROMOS 43B1 force field and Steepest Descent algorithm.

2.3. Detection of physicochemical, pharmacokinetic parameters, and toxicity of ligands.

Physico-chemical properties of the compounds were computed using the Swiss ADME web service. These included their molecular weight, number of heavy atoms, number of heavy aromatic atoms, number of rotatable bonds, number of H bond acceptors, number of H bond donors, molar refractivity, and topological polar surface area (TPSA), an octanol-water partition coefficient (XLogP3).

Pharmacokinetic properties were predicted using the PreADMET online database and Swiss ADME web service. Parameters evaluated included GI absorption, P-gp substrate, BBB permeant, Caco-2 permeability, Lipinski filter, Ghose filter, Veber filter, Egan filter, and Muegge (Bayer) filter.

Toxicity prediction was made by the PreADMET online database. Acute algae toxicity, 2-year carcinogenicity bioassay in mice, acute Daphnia toxicity, and acute fish toxicity were evaluated.

2.4. Protein-ligand docking and energy calculation.

Protein-ligand docking was carried out using Autodock 4.2 software using the protocol elucidated in Ghosh *et al.* [18]. In the first experimental condition, the parent molecule FL and its derivatives FL-D1, FL-D2, FL-D3, FL-D4, FL-D5, FL-D6, FL-D7, FL-D8, FL-D9, and FL-D10 were docked with the energy minimized CDK6 protein molecule using Autodock 4.2. Secondly, DXM was also docked with CDK6 using Autodock 4.2, which is bound to the active site of the protein. The DXM-bound protein structure was again used for docking FL and its derivatives. CDK6 bound DXM was used as a rigid structure. In all experimental conditions, the ligands were kept flexible and were allowed for backbone rotation to ensure maximum degrees of freedom. This condition allows the ligand to explore various conformations of the CDK6 active site in both experimental conditions. While preparing the Autogrid, the size of the grid map was kept to a maximum (i.e., 126 × 126 × 126 with a grid spacing of 0.375 Å). This setting allows the ligand to search for its favorable binding position throughout the protein molecule. For all experimental setups, we used the Lamarckian Genetic Algorithm for docking studies. For each ligand-protein docking output, 10 conformations of the ligand were generated. The ligand binding with the lowest free energy was considered for further analysis in every case. All the docked structures were validated using the online docking server, PatchDock. The docked structures were analyzed through PYMOL (version 2.4.2), Discovery Studio Visualizer (v21.1.0.20298), and LigPlot^{+}. Post docking, all the ligand-bound protein structures were subjected to energy minimization using Discovery Studio 2.5. Energy minimization was done using the steepest descent algorithm, followed by a conjugate gradient algorithm in the presence of the GBSW implicit solvent model and RMS gradient of 0.001 kcal/mol/Å. Protein-ligand binding interaction energy was calculated using the energy minimized structures.

3. Results and Discussion

3.1. Physicochemical properties of ligands.

Physicochemical properties of compounds shown in Fig. 1A were monitored to detect the potential of *in silico* synthesized compounds as drugs, as described in Table 1. There are several approaches to discriminating between drug-like and nondrug-like compounds.

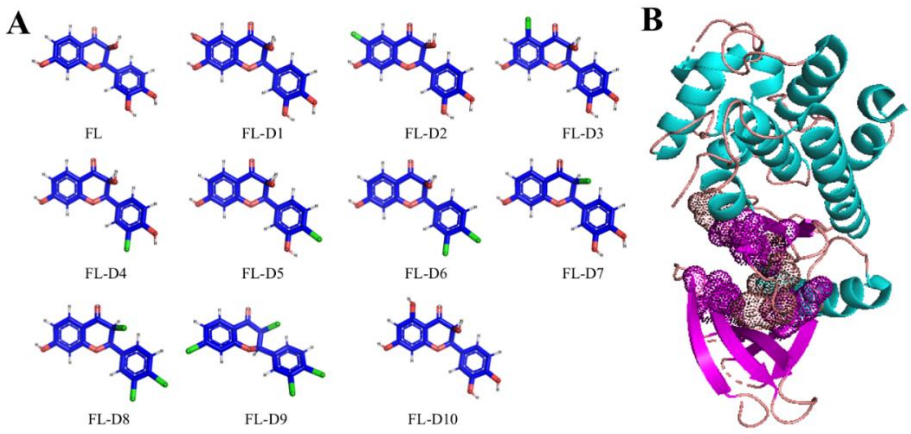

Figure 1. FL and its derivatives with CDK6 protein. A) FL and it's *in silico* synthesized derivatives (FL-D1 to FL-D10). Backbone atoms are blue, hydrogen atoms are gray, oxygen atoms are red, and chlorines are green. B) PDB structure of CDK6. The active site binding pocket is marked in dots.

The molecular weights of the test compounds ranged between 288.25 and 362.03 gm/mol. All the compounds used are within the accepted range of the Lipinski filter [19] and are predicted to be drug-like molecules. The test compounds have 12 heavy aromatic atoms and 3 rings, which conform to Ritchie *et al*. that the presence of more than 3 aromatic rings is associated with poor developability [20]. Ligand affinity decreases by 0.5 kcal for every two rotatable bonds [21]. >10 rotatable bonds are associated with reduced oral activity, although significant deviations have been noted in the literature [22]. All the compounds conform to these constraints. Molar refractivity is an indicator of the overall polarity of a drug and affects its receptor binding, cellular uptake, and bioavailability [23]. The Ghose filter constrains the range of partition coefficient, molar refractivity, molecular weight, and H-bond acceptors [23], and all the compounds fell within a narrow range. TPSA of a molecule, along with hydrogen bond acceptors and hydrogen-bond donors, is a good predictor of the molecule's polarity and, consequently, its transport properties. A general consensus rule for drugs is TPSA < 140 $Å^2$ [24], and the compounds conformed to this constraint. XlogP is the logarithm of the octanol/water partition coefficient and measures a compound's hydrophilicity [25].

Consequently, low hydrophilicity and high logP values are associated with poor absorption or permeation [26]. For compounds to have a good probability of being absorbed, their logP value must not be greater than 5.0. We noted a single slight deviation for FL-D9 in the compound set. From the above results, it can be concluded that most of the *in silico* synthesized molecules have the potency to become potent drug-like molecule(s).

3.2. Pharmacokinetic parameters of ligands.

Pharmacokinetic parameters of compounds were computed to assess the similarity of the test compounds to drugs, details of which are depicted in Table 2. All the compounds have a polar oxygen heterocyclic ring. Heterocyclic rings are common occurrences in small molecule drugs. Their inclusion can modify toxicity/ADME (Absorption, Distribution, Metabolism, and Excretion) properties by changing solubility and lipophilicity polarity, and hydrogen bonding capacity [27].

Table 1. Physico-chemical parameters of the compounds.

Compound Identifier	Formula	Molecular weight g/mol	No. of heavy atoms	No. of aromatic heavy atoms	No. of rotatable bonds	No. of H bond acceptors	No. of H bond doNors	Molar refractivity	TPSA (Topological polar surface area) in Å^2	XLogP3 (OctaNol-water partition co-efficient)
FL	$C_{15}H_{12}O_6$	288.25	21	12	5	6	4	72.73	107.22	0.87
FL-D1	$C_{15}H_{12}O_7$	304.25	22	12	6	7	5	74.76	127.45	0.51
FL-D2	$C_{15}H_{11}ClO_6$	322.7	22	12	5	6	4	77.74	107.22	1.5
FL-D3	$C_{15}H_{11}ClO_6$	322.7	22	12	5	6	4	77.74	107.22	1.38
FL-D4	$C_{15}H_{11}ClO_5$	306.7	21	12	4	5	3	75.72	86.99	1.85
FL-D5	$C_{15}H_{11}ClO_5$	306.7	21	12	4	5	3	75.72	86.99	1.85
FL-D6	$C_{15}H_{10}Cl_2O_4$	325.14	21	12	4	4	2	78.71	66.76	2.84
FL-D7	$C_{15}H_{11}ClO_5$	306.7	21	12	4	5	3	76.37	86.99	2.15
FL-D8	$C_{15}H_9Cl_3O_3$	343.59	21	12	2	3	1	82.34	46.53	4.11
FL-D9	$C_{15}H_8Cl_4O_2$	362.03	21	12	1	2	0	85.33	26.3	5.09
FL-D10	$C_{15}H_{12}O_7$	304.25	22	12	6	7	5	74.76	127.45	0.95

Table 2. Pharmacokinetic properties of the compounds.

Compound Identifier	GI absorption (SwissADME)	P-gp Substrate (SwissADME)	BBB permeant (PreADMET online database)	Caco-2 Permeability (PreADMET online database)	Lipinski filter (SwissADME)	Ghose filter (SwissADME)	Veber filter (SwissADME)	Egan filter (SwissADME)	Muegge(Bayer) filter (SwissADME)
FL	High	No	0.304125	9.56346	Yes	Yes	Yes	Yes	Yes
FL-D1	High	No	0.119389	3.42304	Yes	Yes	Yes	Yes	Yes
FL-D2	High	Yes	0.20412	17.4831	Yes	Yes	Yes	Yes	Yes
FL-D3	High	Yes	0.398665	17.4831	Yes	Yes	Yes	Yes	Yes
FL-D4	High	Yes	0.85566	18.0471	Yes	Yes	Yes	Yes	Yes
FL-D5	High	Yes	0.622355	19.5734	Yes	Yes	Yes	Yes	Yes
FL-D6	High	Yes	1.29154	16.1076	Yes	Yes	Yes	Yes	Yes
FL-D7	High	Yes	1.10126	20.4259	Yes	Yes	Yes	Yes	Yes
FL-D8	High	Yes	2.31875	22.5367	Yes	Yes	Yes	Yes	Yes
FL-D9	High	No	1.78476	48.2307	No	Yes	Yes	Yes	No
FL-D10	High	No	0.166964	3.42307	Yes	Yes	Yes	Yes	Yes

Table 3. Toxicity analysis of compounds obtained from PreADMET online database.

Species	Compound names										
	FL	FL-D1	FL-D2	FL-D3	FL-D4	FL-D5	FL-D6	FL-D7	FL-D8	FL-D9	FL-D10
CarciNo_Mouse	negative	negative	negative	negative	negative	negative	negative	negative	negative	positive	negative
medaka_at	0.109228	0.141104	0.0173358	0.0245055	0.0146031	0.0176173	0.00230739	0.0122395	0.000572743	9.33E-05	0.126642
minNow_ at	0.0531448	0.0607791	0.0152277	0.0152348	0.013926	0.0139496	0.00399016	0.00749092	0.000555129	0.000151068	0.0596272
daphnia_ at	0.264475	0.297821	0.0972735	0.116959	0.0903722	0.0998686	0.0337375	0.0827656	0.016112	0.00610912	0.281157
algae_at	0.0534619	0.0400551	0.0250239	0.0281228	0.0377949	0.0330411	0.0235198	0.0332215	0.0147958	0.00912877	0.0409294

ADME characteristics were predicted using the approach adopted by Diana *et al.* [28]. The results show that GI absorption was significantly high for all compounds. P-glycoproteins (P-gp) are pumps that occur on the surface of the intestinal epithelium. Many compounds were predicted to be P-gp substrates except FL-D1, FL-D9, and FL-D10. However, BBB permeability was predicted using the approach developed by Ma X. *et al*. [26], where the range of permeability is reported between < 0.1 to >2.0 [26]. The test compounds were found to have medium levels of Caco2 cell permeability (the range of which is < 4 to > 70), which indicates a moderate absorption through the intestinal epithelium except for FL-D1 and FL-D10, which would not be efficiently absorbed. All the compounds were also subjected to drug-likeness filters, including Lipinski, Ghose, Veber, Egan, and Muegge (Bayer). Lipinski filter constrains the number of Hydrogen bond acceptors and donors in small molecule drugs [19]. Except for FL-D9 (which has only one deviation), the entire test compound conformed to these requirements. Moreover, almost all the compounds fit into the range of Ghose filter [23], Veber filter [22], Egan filter [29], and Muegge(Bayer) filter (except FL-D9) [30].

3.3. Toxicity analysis of compounds.

The toxicity of *in silico* synthesized compounds was predicted from the PreADMET online database, shown in Table 3. Toxicity prediction was made in mice, Japanese rice fish, small freshwater fishes, daphnia, and algae. Except for FL-D9, the predicted toxicities of the compounds were negative in the mice model, which is significant. A significant fraction of protein-coding genes are similar between mice and humans but may exist in different copy numbers [31]. Based on mice data, toxicity prediction can be made in humans.

Compiling all previous results, we found FL-D9 to have only 1 rotatable bond, and the number of H-bond acceptors and donors were 2 and 0, respectively, TPSA was found to be the smallest (26.3 $Å^2$ only), and XLogP3 is greater than 5. Moreover, FL-D9 fails to qualify Lipinski and Muegge (Bayer) filters and is predicted to be positive in toxicity tests when tested in the mouse model. We, therefore, discarded FL-D9 for further experiments.

3.4. Protein-drugs interaction in the absence of DXM.

The structure of the ligands and the binding pocket of the protein molecule is depicted in Fig. 1A and Fig. 1B, respectively. From Figs. 2, 3, S1, and Tables 4, S1, it is clear that FL and all 10 ligands are interacting extensively with CDK6. Interaction of CDK6 with the ligands was studied using Autodock 4.2 for evaluation of binding affinity and prediction of intermolecular interactions, which was re-confirmed through online docking using PatchDock Server (data not shown).

Hydrophobic interactions similar to that of the parent molecule were predicted for several of the ligands. Hydrophobic interactions are significant in energetically stabilizing ligands within the protein structure. The number of hydrophobic atoms in the active core of the drug-target interface affects the biological activity of the drug lead and modifies its ADME properties. Hydrophobic interaction profiles were analyzed using Ligplot$^+$. Most of the compounds showed similar hydrophobic interactions to FL, and many residues in the core of the active site, including VAL27, ALA41, LYS43, PHE98, GLU99, HIS100, VAL101, ASP163, PHE164, appeared to be conserved in this interaction.

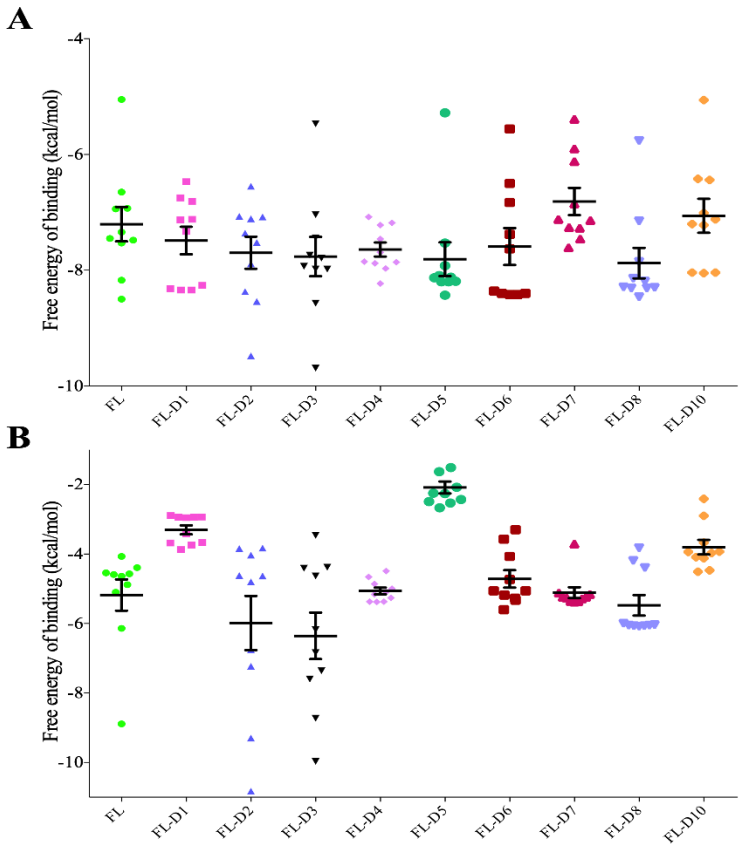

Figure 2. Free energy of binding. Free energy of binding of FL and its derivatives to CDK6 measured by Autodock A) without and B) with DXM.

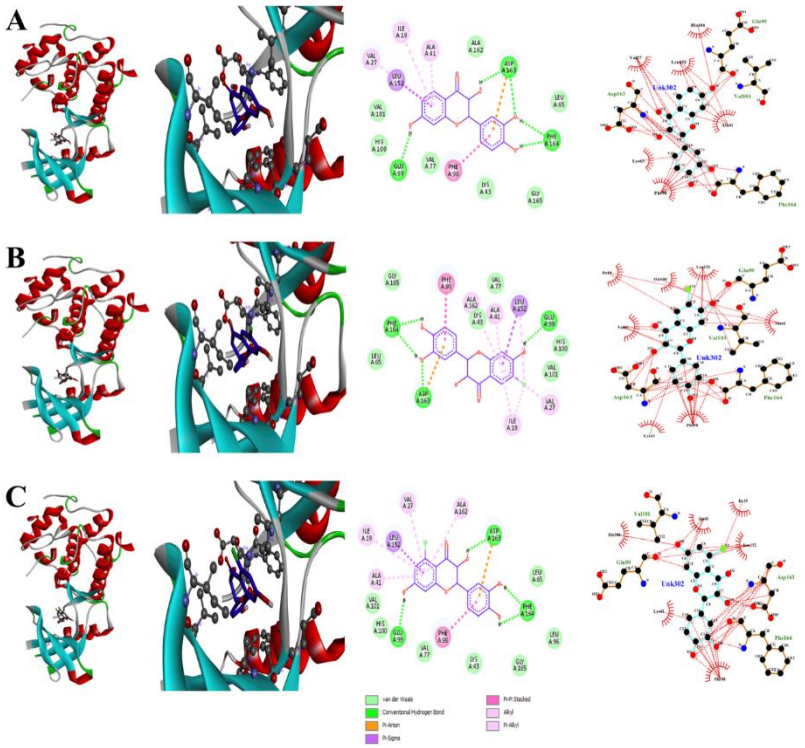

Figure 3. Binding of FL and its derivatives with CDK6 protein. PDB structure of CDK6 (first column), binding of the ligand with CDK6 and amino acids nearby (shown in ball and stick model) to the ligand (shown in stick model) (second column), interactions of CDK6 with ligand were analyzed using Discovery Studio Visualizer (third column), and LigPlot^{+} (fourth column) is shown A) with FL B) with FL-D2 and C) with FL-D3.

Table 4. Interaction of amino acid residues with ligands.

Compound Identifier		Amino Acids having interaction with ligand						
		Hydrophobic Interactions	**Van der Waals**	**H bond**	**Pi-Sigma**	**Pi-Pi Stacked**	**Pi-Alkyl**	**Pi-Anion**
Without Dexamethasone	FL	VAL27, ALA41, LYS43, PHE98, GLU99, HIS100, VAL101, ASP163, PHE164	LYS43, LEU65, VAL77, HIS100, VAL101, ALA162, GLY165	GLU99, ASP163, PHE164	LEU152	PHE98	ILE19, VAL27, ALA41	ASP163
	FL-D1	ILE19, VAL27, ALA41, LYS43, PHE98, GLU99, HIS100, VAL101, ASP163, PHE164	LYS43, LEU65, VAL77, GLY165, HIS100	GLU99, VAL10, ASP163, PHE164,	LEU152	PHE98	ILE19, VAL27, ALA41, ALA162	ASP163
	FL-D2	ILE19, VAL27, ALA41, LYS43, PHE98, GLU99, HIS100, LEU152, ASP163, PHE164	LYS43, LEU65, VAL77, HIS100, VAL101, GLY165	GLU99, ASP163, PHE164	LEU152	PHE98	ILE19, VAL27, ALA41, ALA162	ASP163
	FL-D3	ILE19, ALA41, LYS43, PHE98, GLU99, HIS100, VAL101, LEU152, ASP163, PHE164	LYS43, LEU65, VAL77, LEU96, HIS100, VAL101, GLY165	GLU99, ASP163, PHE164	LEU152	PHE98	ILE19, VAL27, ALA41, ALA162	ASP163
	FL-D4	ILE19, VAL27, ALA41, LYS43, LEU65, VAL77, PHE98, GLU99, HIS100, VAL101, LEU152, ALA162, ASP163, PHE164	VAL27, LEU65, GLU99, HIS100, GLY165	VAL101, PHE164	LEU152	PHE98	ILE19, ALA41, VAL77, ALA162	ASP163
	FL-D5	VAL27, ALA41, LYS43, PHE98, GLU99, HIS100, VAL101, LEU152, ASP153, PHE164	LEU65, VAL77, LEU96, HIS100, VAL101, ALA162	GLU99, ASP163, PHE164	LEU152	-	ILE19, VAL27, ALA41, LYS43, PHE98	ASP163
	FL-D6	GLY20, TYR24, VAL27, ALA41, VAL77, GLU99, HIS100, VAL101, LYS147, GLN149, ASN150, ALA162, ASP163	GLY20, GLU21, LYS43, PHE98, HIS100, VAL101, ASN150	GLU99, ASP163	LEU152	-	VAL27, ALA41, VAL77, LYS147, ALA162	ASP163
	FL-D7	ILE19, VAL27, ALA41, VAL77, PHE98, HIS100, VAL101, ASP163, PHE164	VAL27, LYS43, LEU65, GLN149, ASN150	VAL101, ASP163, PHE164	ILE19, LEU152, ALA162	PHE98	ALA41, VAL77	-
	FL-D8	ILE19, VAL27, ALA41, LYS43, VAL77, PHE98, HIS100, VAL101, LEU152, ALA162, ASP163	LYS43, GLN149, ASN150, PHE164	VAL101	ILE19, LEU152	PHE98, HIS100	VAL27, ALA41, VAL77, ALA162	ASP163
	FL-D10	VAL27, ILE19, VAL27, ALA41, LYS43, PHE98, GLU99, HIS100, LEU152, ASP163, PHE164	LYS43, LEU65, VAL77, LEU96, HIS100, VAL101, ALA162, GLY165	GLU99, ASP163, PHE164	LEU152	PHE98	ILE19, VAL27, ALA41	ASP163

Compound Identifier		Amino Acids having interaction with ligand						
		Hydrophobic Interactions	**Van der Waals**	**H bond**	**Pi-Sigma**	**Pi-Pi Stacked**	**Pi-Alkyl**	**Pi-Anion**
Dexamethasone		ILE19, GLY20, GLU21, TYR24, VAL27, VAL77, PHE98, ASP104, GLN149, ALA162, ASP163	GLY20, ALA41, LYS43, VAL77, PHE98, ASP104, ASN150, LEU152, ALA162, ASP163	TYR24, GLU21, GLN149	-	-	ILE19, VAL27	-
With Dexamethasone	FL	Dexamethasone, ALA17, ILE19, LYS29, ALA41, HIS100, VAL101, ASP102, LEU152	VAL77, GLU99, ASP102, GLN103, ASP104	LYS29	Dexamethasone, ILE19	-	ALA17, ALA41, VAL101, LEU152	LYS29
	FL-D2	Dexamethasone, ILE19, ALA41, HIS100, VAL101, ASP102, GLN103, ASP104, THR107, LEU152	GLY20, VAL77, GLN103	ILE19, GLU99, ASP102, ASP104, THR107	Dexamethasone	-	ALA41, VAL101, LEU152	ASP104
	FL-D3	Dexamethasone, ALA17, ILE19, LYS29, HIS100, VAL101, ASP102, ASP104, LEU152	ALA41, VAL77, GLU99, ASP102, ASP104	VAL101	ILE19	-	Dexamethasone, ALA17, LEU152	-
	FL-D5	Dexamethasone, ILE19, HIS100, VAL101, ASP102, ASP104, THR106, THR107, LEU152	GLU18, HIS100, ASP102, ASP104, THR106, THR107	ILE19, VAL101	-	-	Dexamethasone, LEU152	-
	FL-D1, FL-D4, FL-6, FL-D7, FL-D8, FL-D10	**Binds outside active site**						

Van der Waals interactions are short-range electrostatic interatomic forces. Although weak, they contribute to stabilizing protein-ligand interactions, especially if they occur simultaneously. The test compounds showed significant variability in the Van der Waals interaction profiles reflecting a dynamic interacting surface between the drugs and the active site. LYS43, LEU65, VAL77, HIS100, VAL101, and GLY165 were observed to be commonly involved in Van der Waals's interactions with the ligands.

Hydrogen bonds play a crucial role in determining the specificity of ligand-receptor interactions and stabilization of structures. However, a high number of hydrogen bonds can affect absorption, cell permeability, and brain penetration. Residues GLU99 and ASP163 were found to be frequently involved in H bond formation with the ligands.

Other non-covalent interactions predicted include Pi-Sigma, Pi-Pi Stacked, Pi-Alkyl, and Pi-Anion. Pi-sigma interactions stabilize ligand-receptor binding, and residue LEU152 was implicated in most cases this interaction. Pi-Pi stacking involves attractive, non-covalent interactions between parallelly stacked aromatic rings. These interactions do not alter drugs' structural or functional properties and have been targeted for drug delivery and the design of self-assembling systems. Pi-Pi stacking was predicted in FL, FL-D1, FL-D2, FL-D3, FL-D4, FL-D7, FL-D8, and FL-D10 and almost exclusively mediated by PHE98. Pi-alkyl interactions are attractive and help stabilize the interaction of the pi-electron cloud over an aromatic group with electrons of an alkyl group. Pi-alkyl interactions were predicted in all the compounds and, similar to FL, predominantly involved ILE19, VAL27, and ALA41. Pi-anion interactions are non-covalent attractive forces between electron-deficient pi systems on aromatic molecules and anions. These are also stabilizing forces enabling ligand-receptor interaction. These interactions were observed in FL, FL-D1, FL-D2, FL-D3, FL-D4, FL-D5, FL-D6, FL-D8, and FL-D10 and almost exclusively involved the ASP163 residue.

Free energy of binding of a protein-ligand complex is important as it can give some idea about the stability. If we consider the lowest binding energy of ligands with CDK6, from Fig. 1A and Table S1, it can be predicted that FL-D2, and FL-D3 bind more strongly to the CDK6 pocket than FL. The free energy of binding of FL was -8.5 kcal/mol; whereas, when FL-D2, and FL-D3 bind to CDK6, the free energy of binding was -9.48 kcal/mol and -9.69 kcal/mol, respectively. The whole system energy was also minimized after docking. Free energy of the system when bound to FL, FL-D2, and FL-D3 were -65.3 kcal/mol, -67.6 kcal/mol, and -66.8 kcal/mol, respectively, measured by Discovery Studio 2.5.

3.5. Interaction of DXM with the target protein.

Corticosteroids, including DXM have been employed as an adjuvant in cancer therapy for palliation and immunomodulatory activity but were also reported to cause a G1 cell cycle arrest [32]. Here we have found that DXM can also interact with the CDK6 active site. DXM binds to the active strongly with a free energy of binding of -8.97 kcal/mol. It also forms extensive hydrophobic interactions with ILE19, GLY20, GLU21, TYR24, VAL27, VAL77, PHE98, ASP104, GLN149, ALA162, and ASP163, similar to FL. Van der Waals interactions were predicted to occur with residues GLY20, ALA41, LYS43, VAL77, PHE98, ASP104, ASN150, LEU152, ALA162, and ASP163, which possibly stabilizes DXM in the binding pocket. It was predicted to have H bonding with TYR24, GLU21, and GLN149; pi-alkyl bonding with ILE19 and VAL27. The interaction profile was similar to that of FL, and its derivatives are shown in Fig. 4 and Table 4.

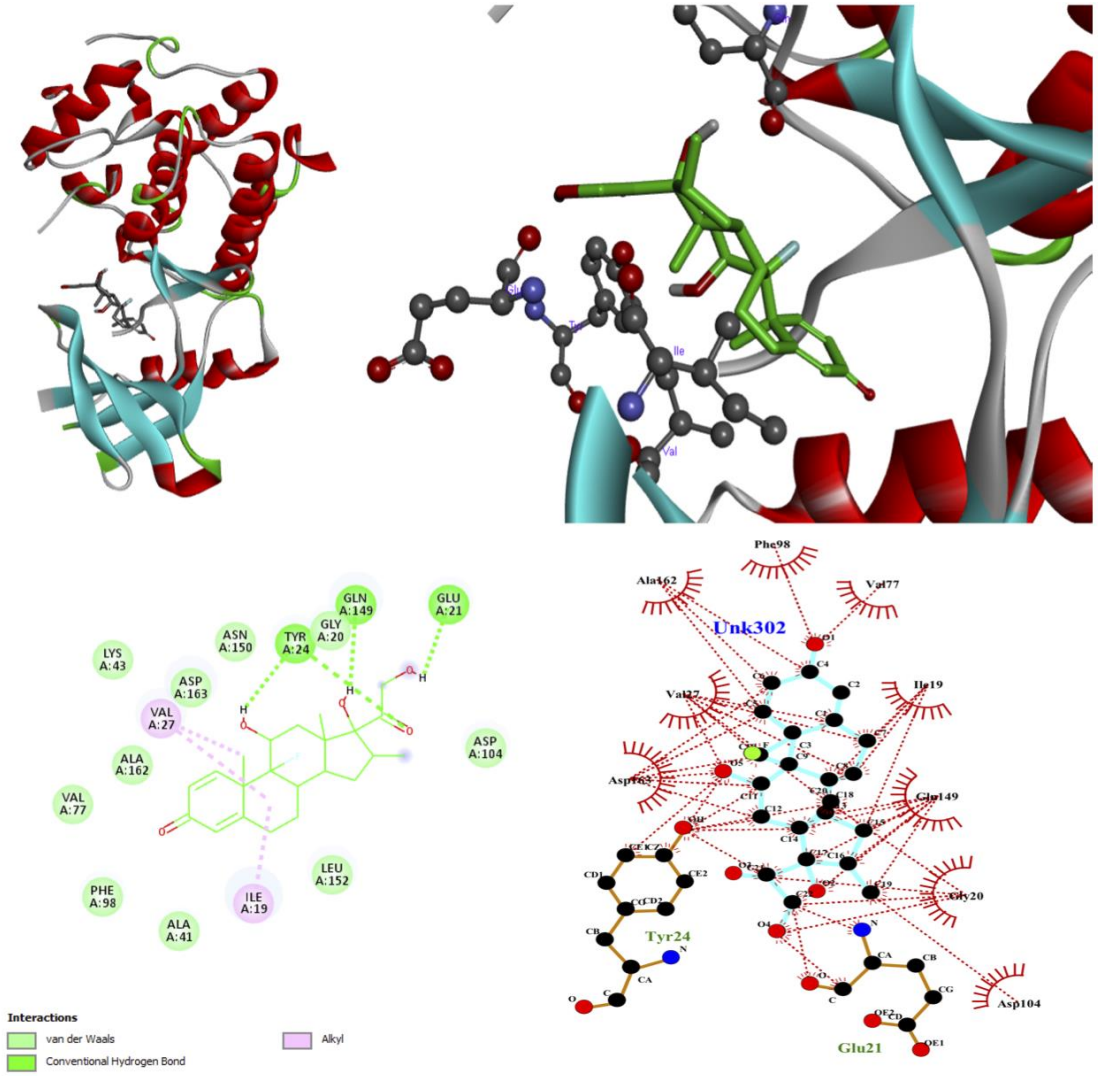

Figure 4. Binding of DXM with CDK6 protein. Binding of DXM (green backbone) with CDK6 (upper left) with amino acids in close proximity (shown in ball and stick model) interacting with DXM (shown in stick model) (upper right). Interactions of CDK6 with DXM were analyzed using Discovery Studio Visualizer (lower left) and LigPlot^{+} (lower right).

3.6. Protein-drugs interaction in the presence of DXM.

We hypothesized that DXM could have a synergistic effect in cancer treatment by CDK6 inhibitors and performed docking simulations of the ligands in the presence of DXM. As outlined in Figs. 5, S2, and Table 4, the parent molecule FL, Fl-D2, Fl-D3, and Fl-D5 were able to bind in the active site. In the presence of DXM, the compounds formed hydrophobic interactions with the CDK6 active site with a significant change in the contact points. For example, hydrophobic interactions of FL-D2 in the DXM involved interactions with residues LYS29, ASP104, and THR107, which were rarely involved without DXM. In addition, the compounds interacted with DXM and possibly stabilized the complex through hydrophobic interaction (FL, FL-D2, FL-D3, and FL-D5), and Pi-Sigma bond (FL and FL-D2), and Pi-Alkyl interaction (FL-D3 and FL-D5).

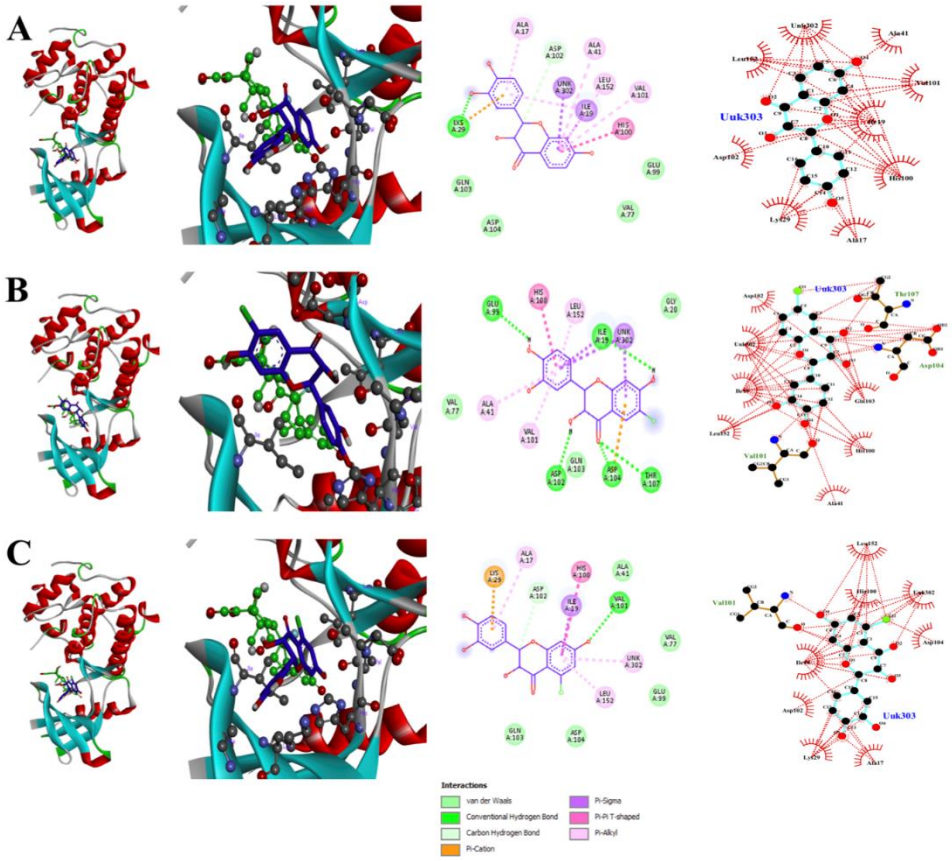

Figure 5. Binding of FL and its derivatives with CDK6 protein in the presence of DXM. PDB structure of CDK6 (first column), binding of ligand with CDK6 and amino acids nearby (shown in ball and stick model) to the ligand (shown in stick model) in the presence of DXM (second column), interactions of CDK6 with ligand were analyzed using Discovery Studio Visualizer (third column) and LigPlot$^+$ (fourth column) is shown A) with FL B) with FL-D2 C) with FL-D3.

Fig. 1B and Table S2 show the binding energy of FL-D2 and FL-D3 predicted to be significantly lower than the parent molecule FL. These were identified as the most viable compounds for further studies. FL-D2 and FL-D3 showed binding energy of -10.83 kcal/mol and -9.97 kcal/mol, respectively, which were lower than FL with and without DXM; i.e., -8.89 kcal/mol and -8.5 kcal/mol, respectively. Free energy of the whole system in the presence of DXM when bound to FL, FL-D2, and FL-D3 were -114.6 kcal/mol, -97.8 kcal/mol, and -115.0 kcal/mol, respectively; which re-confirms the stability of the protein-ligand complexes.

Cyclin-dependent kinases (CDKs) are a family of 13 serine/threonine protein kinases involved in cell cycle regulation [33]. CDK6 phosphorylates retinoblastoma (Rb) proteins [34] from a class of tumor suppressors, inhibiting the transcription factors from binding to their DNA targets; over 100 genes controlling DNA replication, cell cycle progression, DNA damage repair, apoptosis, differentiation, and development. Phosphorylation of Rb proteins in the G1 phase of the cell cycle restricts the cell from entering the S phase.

Dysregulation of CDK6 has been found in more than 80% of human cancers. For example, in the case of T-cell lymphoblastic lymphoma/leukemia, CDK6 overexpression was found in almost all neoplastic lymphoid cells [35]. CDK6 dysregulation has been observed in leukemias involving chromosomal translocations and chromosomal rearrangements [36]. Yang *et al*. observed overexpression of CDK6 were found to impart resistance against CDK6 inhibitors in breast cancer cell lines [37]. CDK6 dysregulation is associated with the pathophysiology of brain cancers [38]. Aberrant CDK6 expression has been associated with

several common oncogenic pathways like the JAK-STAT pathway [39], NF-κB pathway [40], MAPK pathway [41], etc., involving tumorigenesis, which is targeted for therapy.

Several strategies have been developed to target CDK6 for cancer therapy. Chemotherapy and radiotherapy have been used to sensitize cancer cells to inhibit CDK6 function [42–44]. However, safety concerns have limited their use, and many clinical and preclinical studies are underway to assess the safety and establish an effective combination therapy and safe dose regimens. Only 3 specific small molecule CDK6 inhibitors are approved by the FDA for cancer therapy- palbociclib, ribociclib, and abemaciclib [45–47]. However, these molecules have been prone to resistance, especially when used as a monotherapy. Resistance to CDK6 inhibition has emerged due to the vastly interconnected web of signaling mechanisms, which can adapt to the specific conditions prevailing in the cell. These signaling pathways can impart flexibility that can ultimately bypass the requirement for CDK6 expression in cell-cycle regulation [48]. These disadvantages have prompted us to search for alternative safe and effective avenues for CDK6 inhibition.

Flavonoids have been shown to have broad-spectrum health benefits, including anti-oxidative, anti-inflammatory, anti-mutagenic, and anti-carcinogenic properties. FL has been well studied for its anticancer properties in preclinical settings [9] through inhibiting angiogenesis, promoting cell cycle arrest in the G2/M phase, and inducing apoptosis in cancer cells [49].

This study used the *in silico* approach to modify FL to generate a pool of potential CDK6 inhibitors. We generated 10 such molecules, out of which 9 molecules were subsequently docked with CDK6 protein. All of those exhibited an altered binding profile with the active site of CDK6, and their binding energies and ADME properties were investigated. Docking studies revealed 2 molecules (FL-D2 and FL-D3) to have more advantageous binding properties than FL. The binding energies of these compounds were significantly lower than FL, possibly improving their specificity towards CDK6. Further investigation is required in this regard. DXM has been used in cancer palliative care, but the docking studies revealed that it binds to the CDK6 active site. Docking the compounds in the presence of DXM was done to investigate a possible synergistic effect. FL-D2 and FL-D3 were found to have even lower binding energies in the presence of DXM compared to their use in isolation. This supports the possibility of combination therapies using these molecules.

4. Conclusions

CDK6 was targeted for the development of potential anticancer therapeutics. Ten small lead molecules were designed, and the predicted physicochemical properties, pharmacokinetic parameters, and toxicity parameters of nine molecules were within acceptable ranges. Molecular docking and binding free energy calculations revealed two molecules with advantageous properties compared to the established drug FL. The insertion of the chloride group in 4’ or 5’ positions (Fig. 1) of FL was significant. These two conformations allowed the modified flavonoids to bind the active site of CDK6 more strongly than the parent molecule in the presence of DXM. Electrostatic forces and Van der Waals interactions were important factors for stabilizing the complex. These findings are significant as they indicate a platform for quickly generating and screening potential anticancer molecules.

Funding

This research received no external funding.

Acknowledgments

A Bhattacharya and D Guha were supported with the basic facilities from the University of Kalyani and DST-PURSE II, Govt. of India. The authors are also thankful to the University of Kalyani for providing a plagiarism-checking facility.

Conflicts of Interest

The authors declare no conflict of interest.

References

1. Morris, G.M.; Goodsell, D.S.; Halliday, R.S.; Huey, R.; Hart, W.E.; Belew, R.K.; Olson, A.J. Automated docking using a Lamarckian genetic algorithm and an empirical binding free energy function. *Journal of Computational Chemistry* **1998**, *19*, 1639-1662, https://doi.org/10.1002/(SICI)1096-987X(19981115)19:14<1639::AID-JCC10>3.0.CO;2-B.
2. Dong, L.; Qu, X.; Zhao, Y.; Wang, B. Prediction of Binding Free Energy of Protein–Ligand Complexes with a Hybrid Molecular Mechanics/Generalized Born Surface Area and Machine Learning Method. *ACS Omega* **2021**, *6*, 32938-32947, https://doi.org/10.1021/acsomega.1c04996.
3. Mitra, A.; Biswas, R.; Bagchi, A.; Ghosh, R. Insight into the binding of a synthetic nitro-flavone derivative with human poly (ADP-ribose) polymerase 1. *International Journal of Biological Macromolecules* **2019**, *141*, 444-459, https://doi.org/10.1016/j.ijbiomac.2019.08.242.
4. Li, A.; Blow, J.J. The origin of CDK regulation. *Nature Cell Biology* **2001**, *3*, E182-E184, https://doi.org/10.1038/35087119.
5. Tan, C.; Ginzberg, M.B.; Webster, R.; Iyengar, S.; Liu, S.; Papadopoli, D.; Concannon, J.; Wang, Y.; Auld, D.S.; Jenkins, J.L.; Rost, H.; Topisirovic, I.; Hilfinger, A.; Derry, W.B.; Patel, N.; Kafri, R. Cell size homeostasis is maintained by CDK4-dependent activation of p38 MAPK. *Developmental Cell* **2021**, *56*, 1756-1769, https://doi.org/10.1016/j.devcel.2021.04.030.
6. Yuan, K.; Wang, X.; Dong, H.; Min, W.; Hao, H.; Yang, P. Selective inhibition of CDK4/6: A safe and effective strategy for developing anticancer drugs. *Acta Pharmaceutica Sinica B* **2021**, *11*, 30-54, https://doi.org/10.1016/j.apsb.2020.05.001.
7. Kent, L.N.; Leone, G. The broken cycle: E2F dysfunction in cancer. *Nature Reviews Cancer* **2019**, *19*, 326-338, https://doi.org/10.1038/s41568-019-0143-7.
8. Khan, A.U.; Dagur, H.S.; Khan, M.; Malik, N.; Alam, M.; Mushtaque, M. Therapeutic role of flavonoids and flavones in cancer prevention: Current trends and future perspectives. *European Journal of Medicinal Chemistry Reports* **2021**, *3*, https://doi.org/10.1016/j.ejmcr.2021.100010.
9. Kubatka, P.; Mazurakova, A.; Samec, M.; Koklesova, L.; Zhai, K.; Al-Ishaq, R.; Kajo, K.; Biringer, K.; Vybohova, D.; Brockmueller, A.; Pec, M.; Shakibaei, M.; Giordano, F.A.; Büsselberg, D.; Golubnitschaja, O. Flavonoids against non-physiologic inflammation attributed to cancer initiation, development, and progression—3PM pathways. *EPMA Journal* **2021**, *12*, 559-587, https://doi.org/10.1007/s13167-021-00257-y.
10. Susanti, N.M.; Tjahjono, D.H. Cyclin-Dependent Kinase 4 and 6 Inhibitors in Cell Cycle Dysregulation for Breast Cancer Treatment. *Molecules* **2021**, *26*, https://doi.org/10.3390/molecules26154462.
11. Guha, D.; Mukherjee, R.; Aich, P. Macrophage plays important role in cortisol and serotonin induced adipogenesis in vitro. *In Vitro Cellular & Developmental Biology - Animal* **2020**, *56*, 511-521, https://doi.org/10.1007/s11626-020-00482-1.
12. Zhang, Y.; Shi, G.; Zhang, H.; Xiong, Q.; Cheng, F.; Wang, H.; Luo, J.; Zhang, Y.; Shi, P.; Xu, J.; Fu, J.; Chen, N.; Cheng, L.; Li, Y.; Dai, L.; Yang, Y.; Yu, D.; Zhang, S.; Deng, H. Dexamethasone enhances the lung metastasis of breast cancer via a PI3K-SGK1-CTGF pathway. *Oncogene* **2021**, *40*, 5367-5378, https://doi.org/10.1038/s41388-021-01944-w.
13. Bortolozzi, R.; Mattiuzzo, E.; Trentin, L.; Accordi, B.; Basso, G.; Viola, G. Ribociclib, a Cdk4/Cdk6 kinase inhibitor, enhances glucocorticoid sensitivity in B-acute lymphoblastic leukemia (B-All). *Biochemical Pharmacology* **2018**, *153*, 230-241, https://doi.org/10.1016/j.bcp.2018.01.050.
14. Bhattacharya, A.; Guha, D. Chemotherapy or Immunotherapy: A Search for the Potential Anti-Cancer Treatment Strategies. *Int. J. Sci. Res.* **2021**, *10*, 1306–12.

15. Ghosh, R.; Girigoswami, K.; Dipanjan, G. Suppression of apoptosis leads to cisplatin resistance in V79 cells subjected to chronic oxidative stress. *Indian journal of biochemistry & biophysics* **2012**, *49*, 363-370.
16. Guha, D.; Banerjee, A.; Mukherjee, R.; Pradhan, B.; Peneva, M.; Aleksandrov, G.; Suklabaidya, S.; Senapati, S.; Aich, P. A probiotic formulation containing Lactobacillus bulgaricus DWT1 inhibits tumor growth by activating pro-inflammatory responses in macrophages. *Journal of Functional Foods* **2019**, *56*, 232-245, https://doi.org/10.1016/j.jff.2019.03.030.
17. Lu, H.; Chang, D.J.; Baratte, B.; Meijer, L.; Schulze-Gahmen, U. Crystal Structure of a Human Cyclin-Dependent Kinase 6 Complex with a Flavonol Inhibitor, Fisetin. *Journal of Medicinal Chemistry* **2005**, *48*, 737-743, https://doi.org/10.1021/jm049353p.
18. Ghosh, R.; Guha, D.; Bhowmik, S.; Bagchi, A. Possible role of 2, 2'- (Diazinodimethylidyne) di - (o-phenylene) dibenzoate, a novel hydrazine as an anti-HIV agent. *J. Biophys. Struct. Biol.* **2010**, *2*, 42–6.
19. Lipinski, C.A.; Lombardo, F.; Dominy, B.W.; Feeney, P.J. Experimental and computational approaches to estimate solubility and permeability in drug discovery and development settings1PII of original article: S0169-409X(96)00423-1. The article was originally published in Advanced Drug Delivery Reviews 23 (1997) 3–25.1. *Advanced Drug Delivery Reviews* **2001**, *46*, 3-26, https://doi.org/10.1016/S0169-409X(00)00129-0.
20. Ritchie, T.J.; Macdonald, S.J.F. The impact of aromatic ring count on compound developability – are too many aromatic rings a liability in drug design? *Drug Discovery Today* **2009**, *14*, 1011-1020, https://doi.org/10.1016/j.drudis.2009.07.014.
21. Andrews, P.R.; Craik, D.J.; Martin, J.L. Functional group contributions to drug-receptor interactions. *Journal of Medicinal Chemistry* **1984**, *27*, 1648-1657, https://doi.org/10.1021/jm00378a021.
22. Veber, D.F.; Johnson, S.R.; Cheng, H.-Y.; Smith, B.R.; Ward, K.W.; Kopple, K.D. Molecular Properties That Influence the Oral Bioavailability of Drug Candidates. *Journal of Medicinal Chemistry* **2002**, *45*, 2615-2623, https://doi.org/10.1021/jm020017n.
23. Ghose, A.K.; Viswanadhan, V.N.; Wendoloski, J.J. A Knowledge-Based Approach in Designing Combinatorial or Medicinal Chemistry Libraries for Drug Discovery. 1. A Qualitative and Quantitative Characterization of Known Drug Databases. *Journal of Combinatorial Chemistry* **1999**, *1*, 55-68, https://doi.org/10.1021/cc9800071.
24. Matsson, P.; Kihlberg, J. How Big Is Too Big for Cell Permeability? *Journal of Medicinal Chemistry* **2017**, *60*, 1662-1664, https://doi.org/10.1021/acs.jmedchem.7b00237.
25. Cheng, T.; Zhao, Y.; Li, X.; Lin, F.; Xu, Y.; Zhang, X.; Li, Y.; Wang, R.; Lai, L. Computation of Octanol−Water Partition Coefficients by Guiding an Additive Model with Knowledge. *Journal of Chemical Information and Modeling* **2007**, *47*, 2140-2148, https://doi.org/10.1021/ci700257y.
26. Ma, X.-l.; Chen, C.; Yang, J. Predictive model of blood-brain barrier penetration of organic compounds. *Acta Pharmacologica Sinica* **2005**, *26*, 500-512, https://doi.org/10.1111/j.1745-7254.2005.00068.x.
27. Pajouhesh, H.; Lenz, G.R. Medicinal chemical properties of successful central nervous system drugs. *NeuroRX* **2005**, *2*, 541-553, https://doi.org/10.1602/neurorx.2.4.541.
28. Daina, A.; Zoete, V. A BOILED-Egg To Predict Gastrointestinal Absorption and Brain Penetration of Small Molecules. *ChemMedChem* **2016**, *11*, 1117-1121, https://doi.org/10.1002/cmdc.201600182.
29. Egan, W.J.; Merz, K.M.; Baldwin, J.J. Prediction of Drug Absorption Using Multivariate Statistics. *Journal of Medicinal Chemistry* **2000**, *43*, 3867-3877, https://doi.org/10.1021/jm000292e.
30. Muegge, I.; Heald, S.L.; Brittelli, D. Simple Selection Criteria for Drug-like Chemical Matter. *Journal of Medicinal Chemistry* **2001**, *44*, 1841-1846, https://doi.org/10.1021/jm015507e.
31. Chinwalla, A.T.; Cook, L.L.; Delehaunty, K.D.; Fewell, G.A.; Fulton, L.A.; Fulton, R.S.; Graves, T.A.; Hillier, L.W.; Mardis, E.R.; McPherson, J.D.; Miner, T.L.; Nash, W.E.; Nelson, J.O.; Nhan, M.N.; Pepin, K.H.; Pohl, C.S.; Ponce, T.C.; Schultz, B.; Thompson, J.; Trevaskis, E.; Waterston, R.H.; Wendl, M.C.; Wilson, R.K.; Yang, S.-P. ; An, P.; Berry, E.; Birren, B.; Bloom, T.; Brown, D.G.; Butler, J.; Daly, M.; David, R.; Deri, J.; Dodge, S.; Foley, K.; Gage, D.; Gnerre, S.; Holzer, T.; Jaffe, D.B.; Kamal, M.; Karlsson, E.K.; Kells, C.; Kirby, A.; Kulbokas, E.J.; Lander, E.S.; Landers, T.; Leger, J.P.; Levine, R.; Lindblad-Toh, K.; Mauceli, E.; Mayer, J.H.; McCarthy, M.; Meldrim, J.; Meldrim, J.; Mesirov, J.P.; Nicol, R.; Nusbaum, C.; Seaman, S.; Sharpe, T.; Sheridan, A.; Singer, J.B.; Santos, R.; Spencer, B.; Stange-Thomann, N.; Vinson, J.P.; Wade, C.M.; Wierzbowski, J.; Wyman, D.; Zody, M.C.; Birney, E.; Goldman, N.; Kasprzyk, A.; Mongin, E.; Rust, A.G.; Slater, G.; Stabenau, A.; Ureta-Vidal, A.; Whelan, S.; Ainscough, R.; Attwood, J.; Bailey, J.; Barlow, K.; Beck, S.; Burton, J.; Clamp, M.; Clee, C.; Coulson, A.; Cuff, J.; Curwen, V.; Cutts, T.; Davies, J.; Eyras, E.; Grafham, D.; Gregory, S.; Hubbard, T.; Hunt, A.; Jones, M.; Joy, A.; Leonard, S.; Lloyd, C.; Matthews, L.; McLaren, S.; McLay, K.; Meredith, B.; Mullikin, J.C.; Ning, Z.; Oliver, K.; Overton-Larty, E.; Plumb, R.; Potter, S.; Quail, M.; Rogers, J.; Scott, C.; Searle, S.; Shownkeen, R.; Sims, S.; Wall, M.; West, A.P.; Willey, D.; Williams, S.; Abril, J.F.; Guigó, R.; Parra, G.; Agarwal, P.; Agarwala, R.; Church, D.M.; Hlavina, W.; Maglott, D.R.; Sapojnikov, V.; Alexandersson, M.; Pachter, L.; Antonarakis, S.E.; Dermitzakis, E.T.; Reymond, A.; Ucla, C.; Baertsch, R.; Diekhans, M.; Furey, T.S.; Hinrichs, A.; Hsu, F.; Karolchik, D.; Kent, W.J.; Roskin, K.M.; Schwartz, M.S.; Sugnet, C.; Weber, R.J.; Bork, P.; Letunic, I.; Suyama, M.; Torrents, D.; Zdobnov, E.M.; Botcherby, M.; Brown, S.D.; Campbell, R.D.; Jackson, I.; Bray, N.; Couronne, O.; Dubchak, I.; Poliakov, A.; Rubin, E.M.; Brent, M.R.; Flicek, P.; Keibler, E.; Korf, I.;

Batalov, S.; Bult, C.; Frankel, W.N.; Carninci, P.; Hayashizaki, Y.; Kawai, J.; Okazaki, Y.; Cawley, S.; Kulp, D.; Wheeler, R.; Chiaromonte, F.; Collins, F.S.; Felsenfeld, A.; Guyer, M.; Peterson, J.; Wetterstrand, K.; Copley, R.R.; Mott, R.; Dewey, C.; Dickens, N.J.; Emes, R.D.; Goodstadt, L.; Ponting, C.P.; Winter, E.; Dunn, D.M.; von Niederhausern, A.C.; Weiss, R.B.; Eddy, S.R.; Johnson, L.S.; Jones, T.A.; Elnitski, L.; Kolbe, D.L.; Eswara, P.; Miller, W.; O'Connor, M.J.; Schwartz, S.; Gibbs, R.A.; Muzny, D.M.; Glusman, G.; Smit, A.; Green, E.D.; Hardison, R.C.; Yang, S.; Haussler, D.; Hua, A.; Roe, B.A.; Kucherlapati, R.S.; Montgomery, K.T.; Li, J.; Li, M.; Lucas, S.; Ma, B.; McCombie, W.R.; Morgan, M.; Pevzner, P.; Tesler, G.; Schultz, J.; Smith, D.R.; Tromp, J.; Worley, K.C.; Lander, E.S.; Abril, J.F.; Agarwal, P.; Alexandersson, M.; Antonarakis, S.E.; Baertsch, R.; Berry, E.; Birney, E.; Bork, P.; Bray, N.; Brent, M.R.; Brown, D.G.; Butler, J.; Bult, C.; Chiaromonte, F.; Chinwalla, A.T.; Church, D.M.; Clamp, M.; Collins, F.S.; Copley, R.R.; Couronne, O.; Cawley, S.; Cuff, J.; Curwen, V.; Cutts, T.; Daly, M.; Dermitzakis, E.T.; Dewey, C.; Mouse Genome Sequencing, C.; Genome Sequencing, C.; Whitehead Institute, M.I.T.C.f.G.R.; European Bioinformatics, I.; Wellcome Trust Sanger, I.; Research Group in Biomedical, I.; Bioinformatics; National Center for Biotechnology, I.; Department of, M.; Division of Medical, G.; Center for Biomolecular, S.; Engineering; Embl; Consortium, U.M.M.S.; Lawrence Berkeley National, L.; Department of Computer, S.; School of Computer, S.; The Jackson, L.; Laboratory for Genome, E.; Affymetrix, I.; Departments of, S.; Health Evaluation, S.; National Human Genome Research, I.; Wellcome Trust Centre for Human, G.; Department of Electrical, E.; Department of Human, A.; Genetics; Department of Human, G.; Howard Hughes Medical, I.; Department of, G.; Departments of, B.; Molecular, B.; Computer, S.; Engineering; Department of Computer, S.; Engineering; Baylor College of, M.; The Institute for Systems, B.; Department of, B.; Molecular, B.; Howard Hughes Medical, I.; Department of, C.; Biochemistry; Departments of, G.; Medicine; Harvard-Partners Center for, G.; Genomics; Department of, S.; Institute, U.D.J.G.; Cold Spring Harbor, L.; Wellcome, T.; Max Planck Institute for Molecular, G.; Genome Therapeutics, C.; Bioinformatics Solutions, I.; Department of, M.; Human, G.; Department of, B.; Members of the Mouse Genome Analysis, G. Initial sequencing and comparative analysis of the mouse genome. *Nature* **2002**, *420*, 520-562, https://doi.org/10.1038/nature01262.
32. Chen, D.-Y.; Lin, C.-C.; Chen, Y.-M.; Chao, Y.-H.; Yang, D.-H. Dextromethorphan Exhibits Anti-inflammatory and Immunomodulatory Effects in a Murine Model of Collagen-Induced Arthritis and in Human Rheumatoid Arthritis. *Scientific Reports* **2017**, *7*, https://doi.org/10.1038/s41598-017-11378-8.
33. Bazzi, Z.A.; Tai, I.T. CDK10 in Gastrointestinal Cancers: Dual Roles as a Tumor Suppressor and Oncogene. *Frontiers in Oncology* **2021**, *11*, https://doi.org/10.3389/fonc.2021.655479.
34. Roufayel, W.; Mezher, R.; Storey, K.B. The Role of Retinoblastoma Protein in Cell Cycle Regulation: An Updated Review. *Current molecular medicine* **2021**, *21*, 620-629, https://doi.org/10.2174/1566524020666210104113003.
35. Chilosi, M.; Doglioni, C.; Yan, Z.; Lestani, M.; Menestrina, F.; Sorio, C.; Benedetti, A.; Vinante, F.; Pizzolo, G.; Inghirami, G. Differential expression of cyclin-dependent kinase 6 in cortical thymocytes and T-cell lymphoblastic lymphoma/leukemia. *Am J Pathol* **1998**, *152*, 209-217.
36. Corcoran, M.M.; Mould, S.J.; Orchard, J.A.; Ibbotson, R.E.; Chapman, R.M.; Boright, A.P.; Platt, C.; Tsui, L.C.; Scherer S.W.; Oscier, D.G. Dysregulation of cyclin dependent kinase 6 expression in splenic marginal zone lymphoma through chromosome 7q translocations. *Oncogene*. **1999**, *18*, 6271–7, https://doi.org/10.1038/sj.onc.1203033.
37. Yang, C.; Li, Z.; Bhatt, T.; Dickler, M.; Giri, D.; Scaltriti, M.; Baselga, J.; Rosen, N.; Chandarlapaty, S. Acquired CDK6 amplification promotes breast cancer resistance to CDK4/6 inhibitors and loss of ER signaling and dependence. *Oncogene* **2017**, *36*, 2255-2264, https://doi.org/10.1038/onc.2016.379.
38. Lu, Y.C. Knockdown of CDK6 enhances glioma sensitivity to chemotherapy. *Oncol. Rep*. **2012**, *28*, 909-14, https://doi.org/10.3892/or.2012.1884.
39. Leslie, K.; Lang, C.; Devgan, G.; Azare, J.; Berishaj, M.; Gerald, W.; Kim, W.B.; Paz, K.; Darnell, J.E.; Albanese, C.; Sakamaki, T.; Pestell, R.; Bromberg, J. Cyclin D1 Is Transcriptionally Regulated by and Required for Transformation by Activated Signal Transducer and Activator of Transcription 3. *Cancer Res.* **2006**, *66*, 2544–52, https://doi.org/10.1158/0008-5472.CAN-05-2203.
40. Barbara, M.; Tania, B.; Sebastian, K.; Veronika, S.; Michaela, P.-M. Inducible deletion of CDK4 and CDK6 – deciphering CDK4/6 inhibitor effects in the hematopoietic system. *Haematologica* **2020**, *106*, 2624-2632, https://doi.org/10.3324/haematol.2020.256313.
41. Scheiblecker, L.; Kollmann, K.; Sexl, V. CDK4/6 and MAPK—Crosstalk as Opportunity for Cancer Treatment. *Pharmaceuticals* **2020**, *13*, https://doi.org/10.3390/ph13120418.
42. Ettl, T.; Schulz, D.; Bauer, R.J. The Renaissance of Cyclin Dependent Kinase Inhibitors. *Cancers* **2022**, *14*, https://doi.org/10.3390/cancers14020293.
43. Whittaker, S.; Madani, D.; Joshi, S.; Chung, S.A.; Johns, T.; Day, B.; Khasraw, M.; McDonald, K.L. Combination of palbociclib and radiotherapy for glioblastoma. *Cell Death Discovery* **2017**, *3*, https://doi.org/10.1038/cddiscovery.2017.33.
44. Whiteway, S.L.; Harris, P.S.; Venkataraman, S.; Alimova, I.; Birks, D.K.; Donson, A.M.; Foreman, N.K.; Vibhakar, R. Inhibition of cyclin-dependent kinase 6 suppresses cell proliferation and enhances radiation

sensitivity in medulloblastoma cells. *Journal of Neuro-Oncology* **2013**, *111*, 113-121, https://doi.org/10.1007/s11060-012-1000-7.
45. George, M.A.; Qureshi, S.; Omene, C.; Toppmeyer, D.L.; Ganesan, S. Clinical and Pharmacologic Differences of CDK4/6 Inhibitors in Breast Cancer. *Frontiers in Oncology* **2021**, *11*, https://doi.org/10.3389/fonc.2021.693104.
46. Martin, M.; Garcia-Saenz, J.A.; Manso, L.; Llombart, A.; Cassinello, A.; Atienza, M.; Ringeisen, F.; Ciruelos, E. Abemaciclib, a CDK4 and CDK6 inhibitor for the treatment of metastatic breast cancer. *Future Oncology* **2020**, *16*, 2763-2778, https://doi.org/10.2217/fon-2020-0604.
47. Osipov, A.; Saung, M.T.; Zheng, L.; Murphy, A.G. Small molecule immunomodulation: the tumor microenvironment and overcoming immune escape. *Journal for ImmunoTherapy of Cancer* **2019**, *7*, https://doi.org/10.1186/s40425-019-0667-0.
48. Ettl, T.; Schulz, D.; Bauer, R.J. The Renaissance of Cyclin Dependent Kinase Inhibitors. *Cancers (Basel)* **2022**, *14*, https://doi.org/10.3390/cancers14020293.
49. Imran, M.; Saeed, F.; Gilani, S.A.; Shariati, M.A.; Imran, A.; Afzaal, M.; Atif, M.; Tufail, T.; Anjum, F.M. Fisetin: An anticancer perspective. *Food Science & Nutrition* **2021**, *9*, 3-16, https://doi.org/10.1002/fsn3.1872.

Supplementary Data

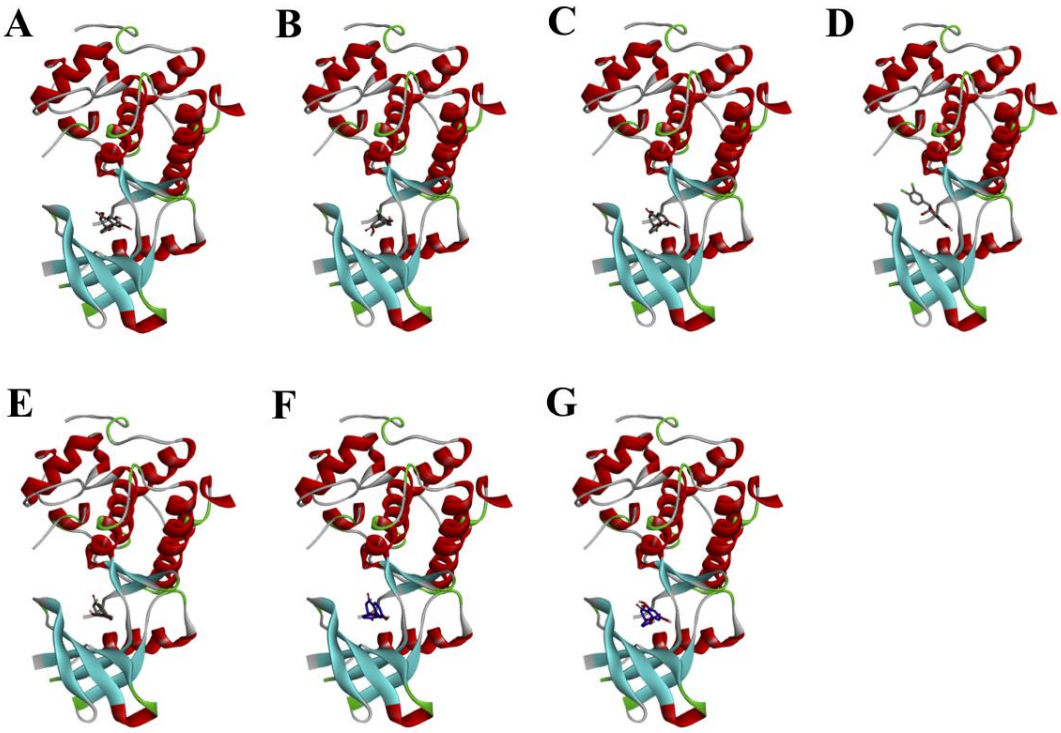

Figure S1. Binding of FL and its derivatives with CDK6. Derivatives of FL A) FL-D1, B) FL-D4, C) FL-D5, D) FL-D6, E) FL-D7, F) FL-D8, and G) FL-D10 after docking with CDK6.

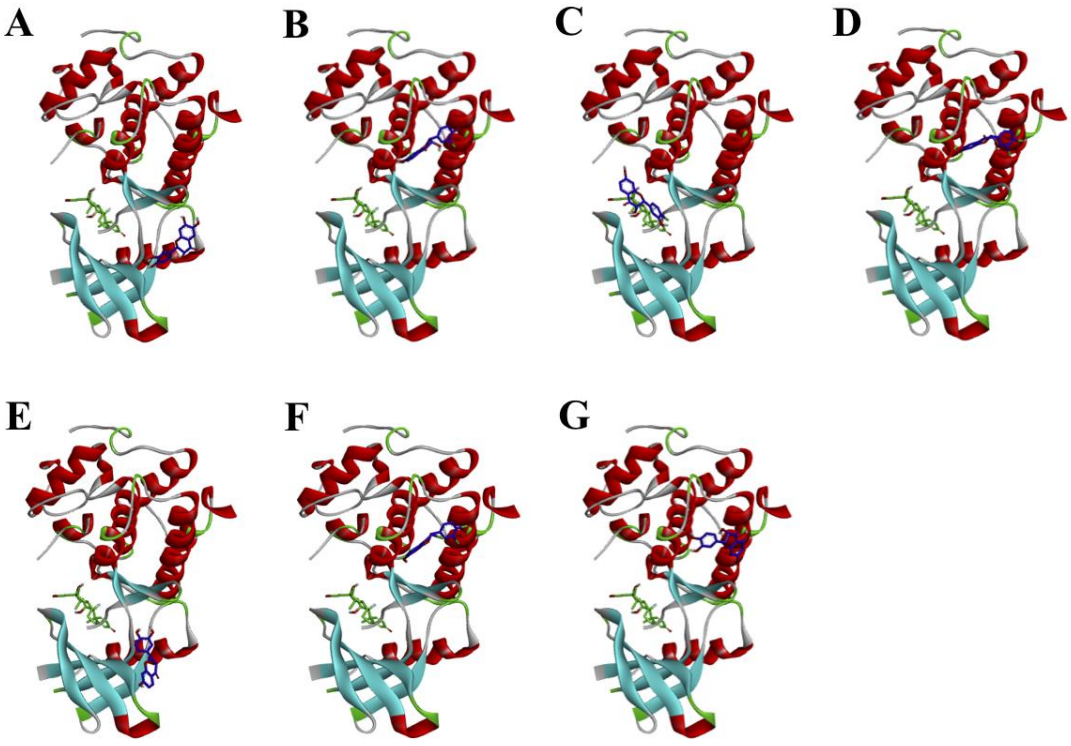

Figure S2. Binding of FL and its derivatives with CDK6 in the presence of DXM. Derivatives of FL A) FL-D1, B) FL-D4, C) FL-D5, D) FL-D6, E) FL-D7, F) FL-D8, and G) FL-D10 after docking with CDK6 in the presence of DXM.

Table S1. Best 10 free energy of binding of the compounds.

Compound Identifier	Free energy of binding (kcal/mol)									
FL	-5.05	-7.53	-6.65	-6.94	-6.93	-7.45	-8.17	-7.48	-7.34	-8.5
FL-D1	-8.32	-7.33	-7.13	-8.26	-7.12	-8.34	-8.34	-6.47	-6.75	-6.81
FL-D2	-7.52	-6.55	-7.89	-7.08	-8.37	-7.07	-8.54	-9.48	-7.11	-7.36
FL-D3	-7.79	-7.04	-5.47	-7.44	-7.98	-8.57	-7.98	-7.74	-9.69	-7.93
FL-D4	-7.08	-8.23	-7.22	-7.18	-7.85	-7.46	-7.88	-7.97	-7.86	-7.69
FL-D5	-8.2	-8.13	-8.09	-5.28	-8.12	-8.43	-8.19	-7.92	-7.53	-8.2
FL-D6	-8.4	-6.83	-5.56	-7.38	-8.42	-8.4	-8.36	-7.63	-8.42	-6.5
FL-D7	-7.61	-7.27	-7.26	-7.14	-7.46	-5.9	-5.39	-6.12	-7.12	-6.85
FL-D8	-8.19	-8.46	-7.85	-7.15	-8.29	-8.31	-8.14	-5.76	-8.31	-8.3
FL-D10	-6.42	-7.01	-7.22	-5.06	-8.05	-8.04	-8.04	-6.44	-7.2	-7.12

Table S2. Best 10 free energy of binding of the compounds in presence of Dexamethasone.

Compound Identifier	Free energy of binding (kcal/mol)									
FL+DXM	-5.1	-4.88	-4.59	-4.57	-4.39	-4.07	-4.64	-4.54	-6.14	-8.89
FL-D1+DXM	-3.87	-3.74	-3.68	-3.67	-3.42	-2.95	-2.94	-2.94	-2.93	-2.89
FL-D2+DXM	-4.8	-4.03	-4.63	-4.62	-7.23	-3.84	-3.83	-6.76	-9.3	-10.83
FL-D3+DXM	-4.63	-4.41	-4.38	-7.6	-7.36	-6.18	-6.84	-3.46	-9.97	-8.73
FL-D4+DXM	-5.38	-5.37	-5.37	-5.26	-5.16	-5.09	-4.86	-5	-4.66	-4.49
FL-D5+DXM	-2.67	-2.53	-1.51	-2.49	-2.43	-2.26	-2.25	-2.08	-1.63	-0.99
FL-D6+DXM	-5.6	-5.33	-5.27	-5.06	-5.18	-5.06	-4.73	-4.07	-3.57	-3.3
FL-D7+DXM	-5.38	-5.37	-5.36	-5.28	-5.26	-5.24	-5.24	-5.16	-5.12	-3.71
FL-D8+DXM	-6.08	-6.07	-6.07	-6.05	-6.05	-6.04	-6	-4.39	-4.19	-3.82
FL-D10+DXM	-4.51	-4.47	-3.94	-3.93	-3.67	-4.12	-4.09	-3.97	-2.9	-2.41